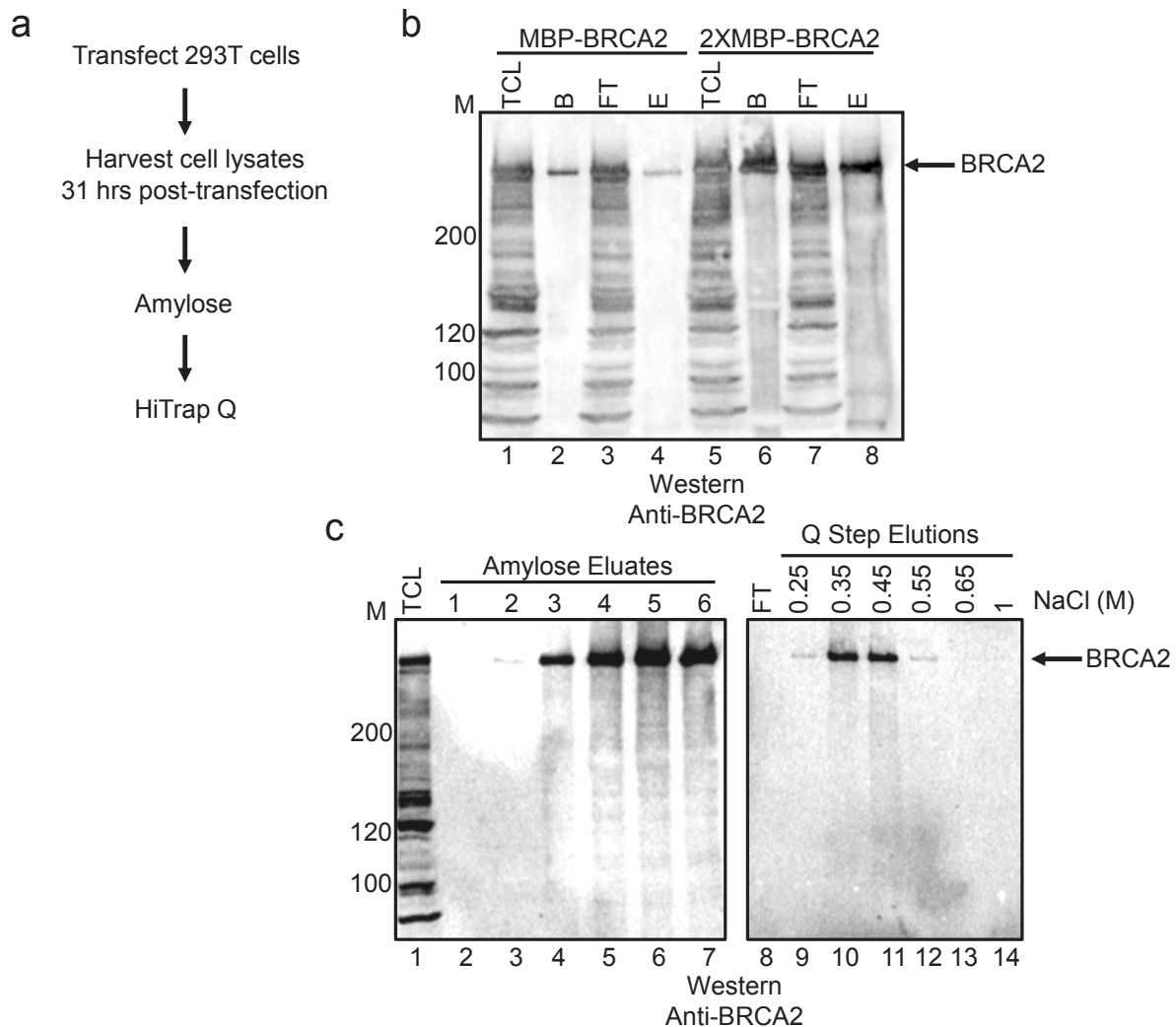


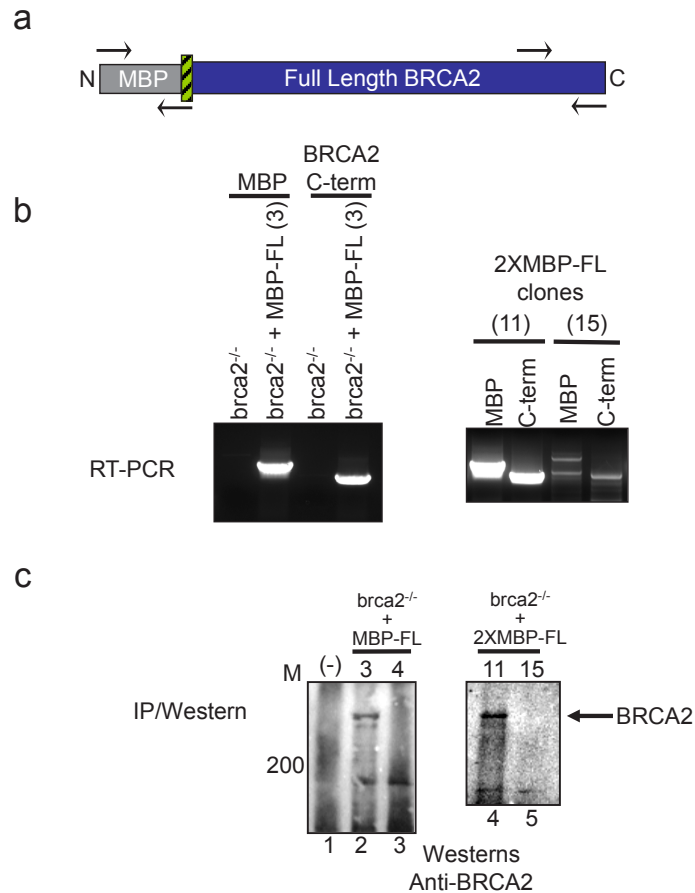
Supplementary Figure 1. Model depicting the functions of BRCA2 in recombinational DNA repair. (a) A DSB generated by either exogenous (*e.g.*, ionizing radiation) or endogenous (*e.g.*, metabolic byproducts) sources is resected to reveal 3' ssDNA tails which *in vivo* are immediately coated by the ssDNA-binding protein, RPA. As more clearly illustrated in panel b, BRCA2 may then bind either at the ss/dsDNA junction or along the ssDNA region. BRCA2 promotes RAD51 filament formation by loading RAD51 onto the RPA-coated ssDNA tail and also by limiting the assembly of RAD51 onto dsDNA. Because BRCA2 inhibits the ATPase activity of RAD51, the filament on ssDNA is stabilized as the active ATP-bound form of RAD51, allowing subsequent filament extension. The RAD51 nucleoprotein filament finds DNA

sequence homology in a donor duplex DNA and promotes DNA strand invasion to form a joint molecule. Completion of DNA DSB repair is then facilitated by multiple proteins acting at several subsequent steps, resulting in a repaired chromosome with genetic information intact.

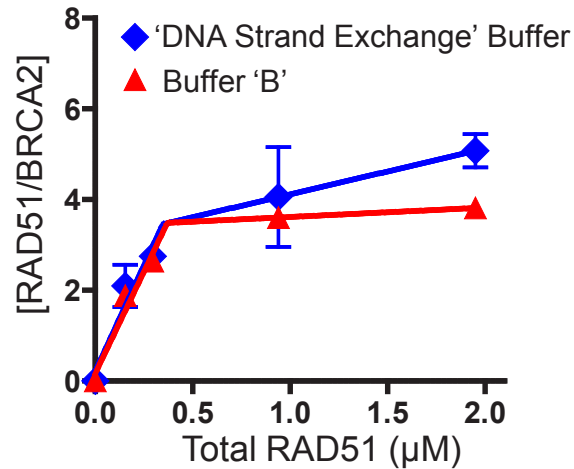
(b) Results from this study also reveal a potential role for BRCA2 in ssDNA gap repair, involving gaps such as those encountered during DNA replication of a damaged template. In this scenario, RPA would bind the ssDNA gap flanked by the two regions of dsDNA. BRCA2 could then bind at either DNA junction or along the ssDNA, and deliver RAD51 to the ssDNA gap. Formation of a continuous RAD51 filament by growth in either the 3' or 5' direction would then allow DNA pairing into the homologous dsDNA template, with possible dissociation of BRCA2 from the ssDNA region, followed by the subsequent steps described in (a) resulting in DNA gap repair and replication restart.



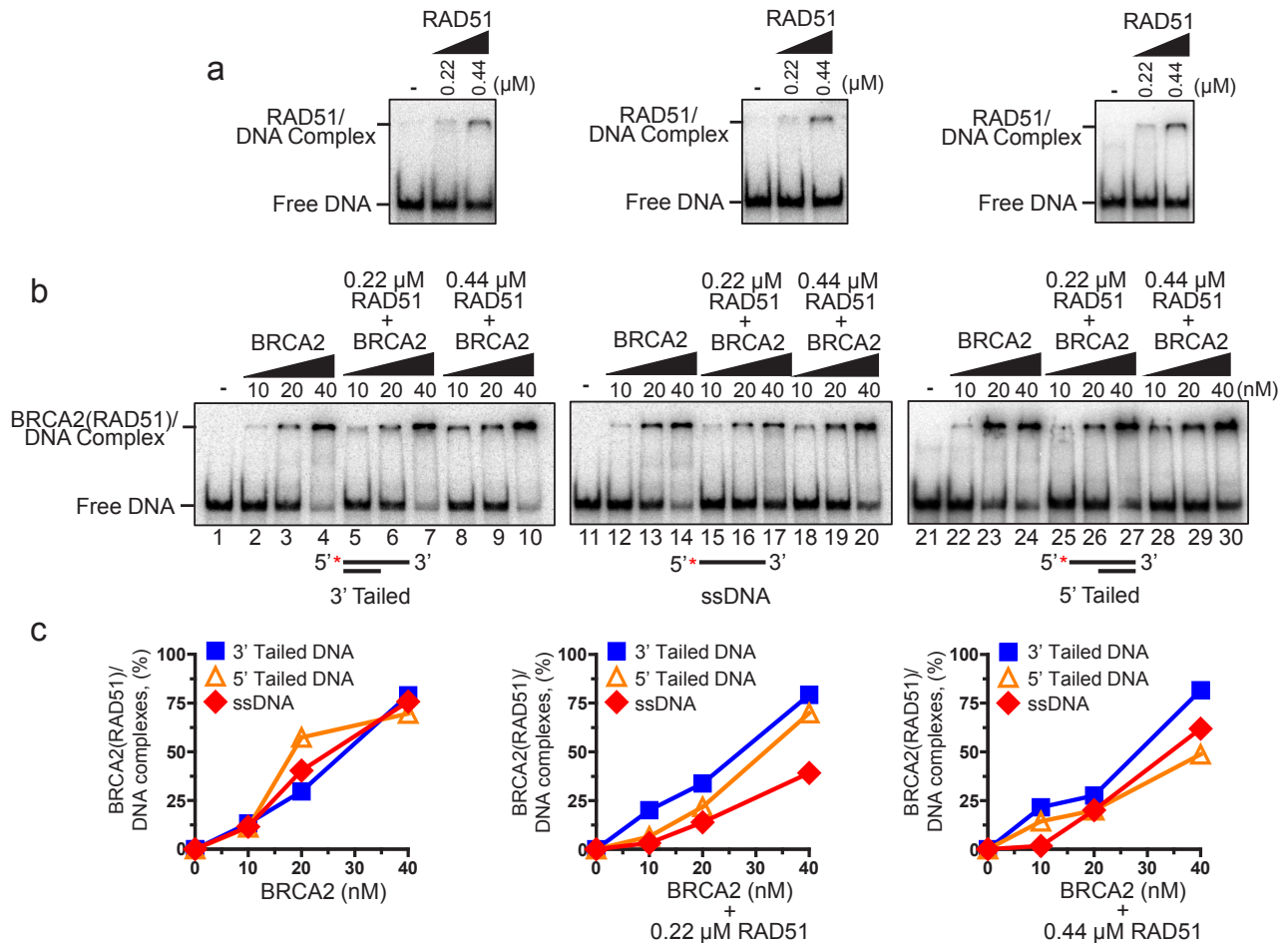
Supplementary Figure 2. Purification of MBP tagged full length BRCA2. (a) Schematic of strategy used to purify full length human BRCA2 with two tandem repeats of MBP tag at the N-terminus (2XMBP-BRCA2). (b) Western blot (6% SDS-PAGE) using an antibody specific for the carboxy-terminus of BRCA2 showing amylose resin purification of either a single MBP tag fused to the N-terminus of BRCA2 (lanes 1-4) or a double MBP tag at the N-terminus of BRCA2 (lanes 5-8). Lanes 1 & 5: TCL = total cellular lysate. Lanes 2 & 6: B = beads. Remaining BRCA2 bound to amylose beads after maltose elution. Lanes 3 & 7: FT = flow-through (unbound) BRCA2. Lanes 4 & 8: E = eluate. Maltose eluates demonstrate the increased yield of BRCA2 with tandem MBP tag. (c) Amylose resin purification of 2XMBP-BRCA2, followed by NaCl step elutions off the HiTrapQ column. Western blot (6% SDS-PAGE) using the same BRCA2 antibody as in (b). TCL = total cell lysate. Amylose resin eluates (lanes 3-6) were pooled before loading onto the HiTrapQ column.



Supplementary Figure 3. Confirmation of stable MBP-BRCA2 expression in *brca2* mutant (VC8) cells by RT-PCR and western blotting. (a) Two sets of primer pairs designed to target and amplify either the MBP tag on the N-terminus of BRCA2 or the C-terminal BRCA2 sequence. (b) Total RNA was isolated from G418-resistant *brca2* mutant cells stably transfected with MBP-BRCA2, 2XMBP-BRCA2, or empty vector and utilized in an RT-PCR strategy as depicted in (a) to screen for clones expressing only full length MBP-tagged BRCA2. The ethidium bromide stained gel on the right demonstrates one clone (11) positive for PCR amplification at both ends of the BRCA2 cDNA, while clone (15) is negative. (c) Clones deemed positive by RT-PCR screening were further tested for protein expression by immunoprecipitation of BRCA2 from cellular lysates (using Ab-1), followed by western blotting to detect recombinant BRCA2 expression (using Ab-2). Lane 1 (-) represents the *brca2* mutant cells (VC8) transfected with empty vector. Clone 3 (lane 2) was positive for recombinant MBP-BRCA2 expression while clone 4 (lane 3) was negative. Clone 11 (lane 4) was positive for 2XMBP-BRCA2 expression while clone 15 (lane 5) was negative, as expected from the RT-PCR results. Clones 3 (MBP-BRCA2) and 11 (2XMBP-BRCA2) were used in the clonogenic survival assay to assess complementation in Figure 1b.



Supplementary Figure 4. The binding of RAD51 to BRCA2 under conditions used for DNA strand exchange assays. 2XMBP-BRCA2 was incubated with increasing amounts of purified RAD51 and the complexes were analyzed with the pull-down assay as described for Figures 1e & f, using either DNA strand exchange buffer (\blacklozenge) or buffer B (\blacktriangle). The data were fit to a segmental linear regression (Prism 5.0b), as described in Figure 1f. For the experiments in DNA strand exchange buffer, the error bars represent S.D. for two independent experiments. For the control, in buffer B, one experiment was conducted and no error bars are shown; however, the reproducibility of similar experiments (*e.g.*, Figure 1), the variation is approximately $\pm 15\%$. The BRCA2 preparation used in this pull-down analysis is slightly less active than the preparations used in the main body of the paper, accounting for the minor decrease in binding demonstrated in buffer B. The binding stoichiometry at the intersection of the two lines is 3.5 ± 1.0 RAD51 per BRCA2 for both solution conditions.



Supplementary Figure 5. The binding of BRCA2 to DNA is unaltered by preincubation

with RAD51. (a) EMSA analyses of RAD51 complexes binding (from left to right): 3' Tailed

DNA, ssDNA, or 5' Tailed DNA. Turnover by RAD51 results in less than 100% of the DNA

persisting as a complex. (b) EMSA analyses of BRCA2-RAD51 complexes binding to: 3'

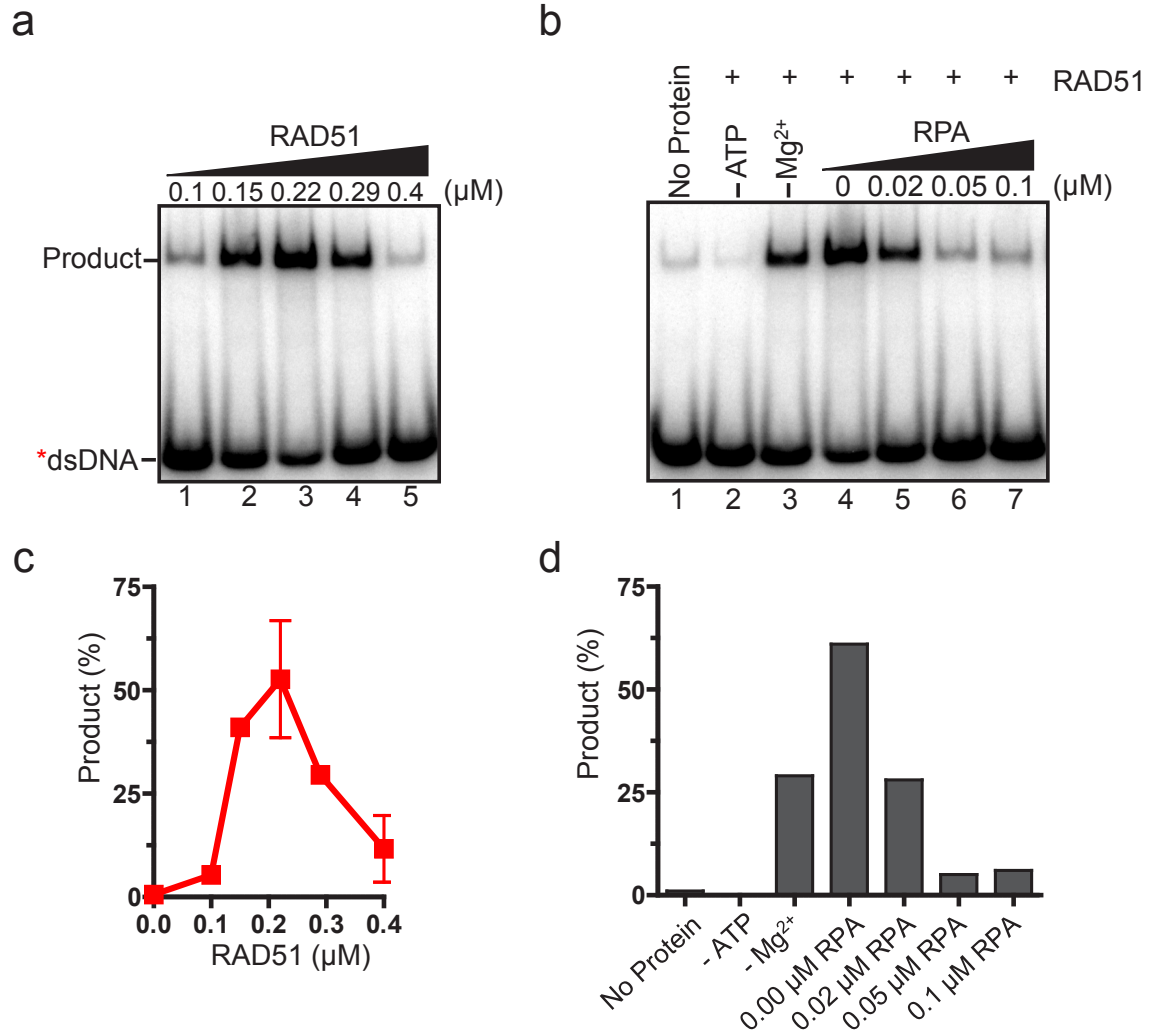
Tailed DNA, ssDNA, or 5' Tailed DNA. (c) Quantification of the EMSA results in (b): 3' Tailed

DNA (■), ssDNA (◆), or 5' Tailed DNA (△). These results are based on a single

experiment and the differences for any of the BRCA2-RAD51-DNA complexes are not

considered to be statistically significant based on typical gel to gel variation observed (*e.g.*,

Figure 2).



Supplementary Figure 6. Optimization of the DNA strand exchange reaction. (a)

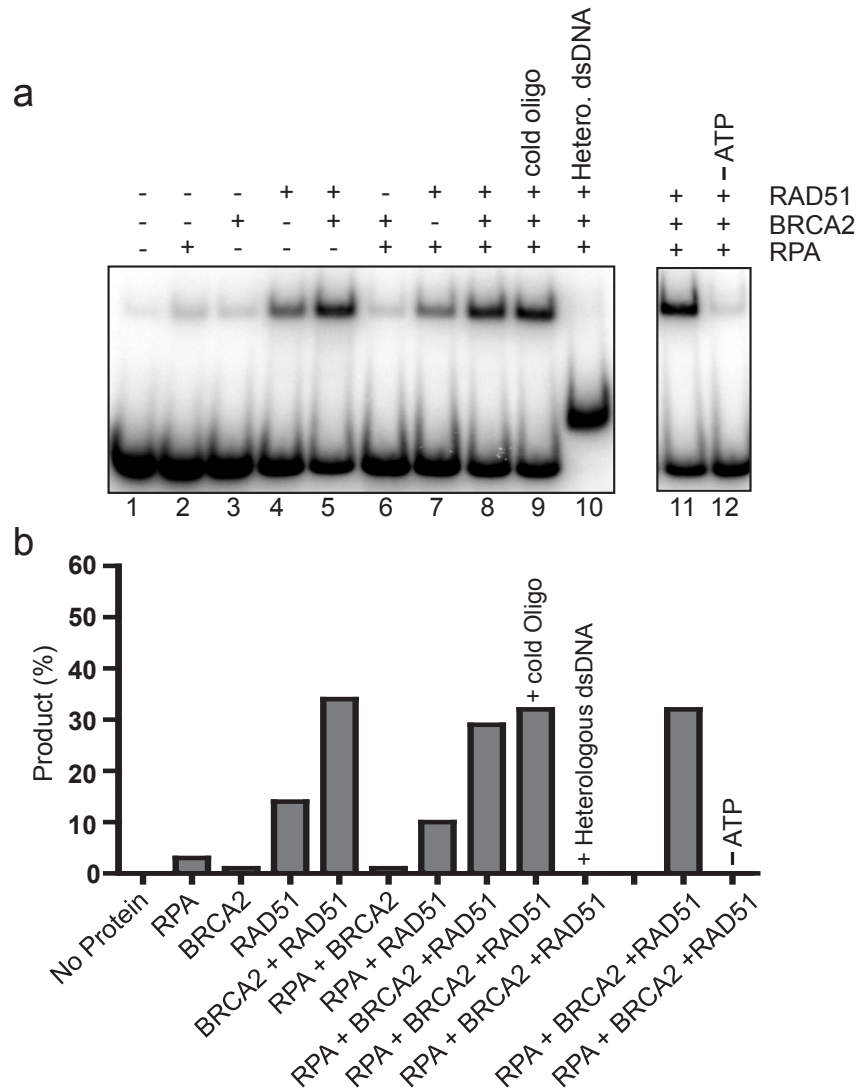
Autoradiogram of DNA strand exchange reactions utilizing the 3' tailed DNA substrate at different concentrations of RAD51 (lanes 1-5). **(b)** Autoradiogram showing DNA strand exchange reactions using the 3' tailed DNA substrate in the presence of 0.22 μM RAD51 (lanes 2-7).

Standard DNA strand exchange buffer, which contains 2 mM CaCl₂, was used. Lane 1: No protein control. Lane 2: ATP omitted. Lane 3: Mg²⁺ omitted. Lanes 4-7: increasing amounts of RPA

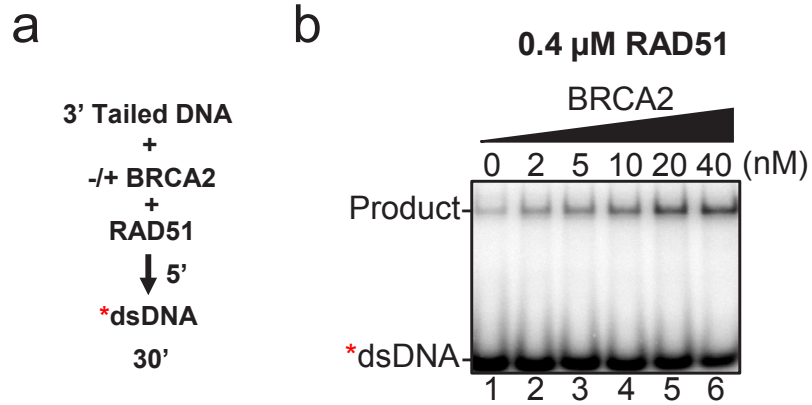
were incubated with the DNA substrate for 5 minutes at 37 °C prior to the addition of RAD51. **(c)**

Quantification of the data in (a) indicating that optimal exchange occurs at 0.22 μM RAD51. Error

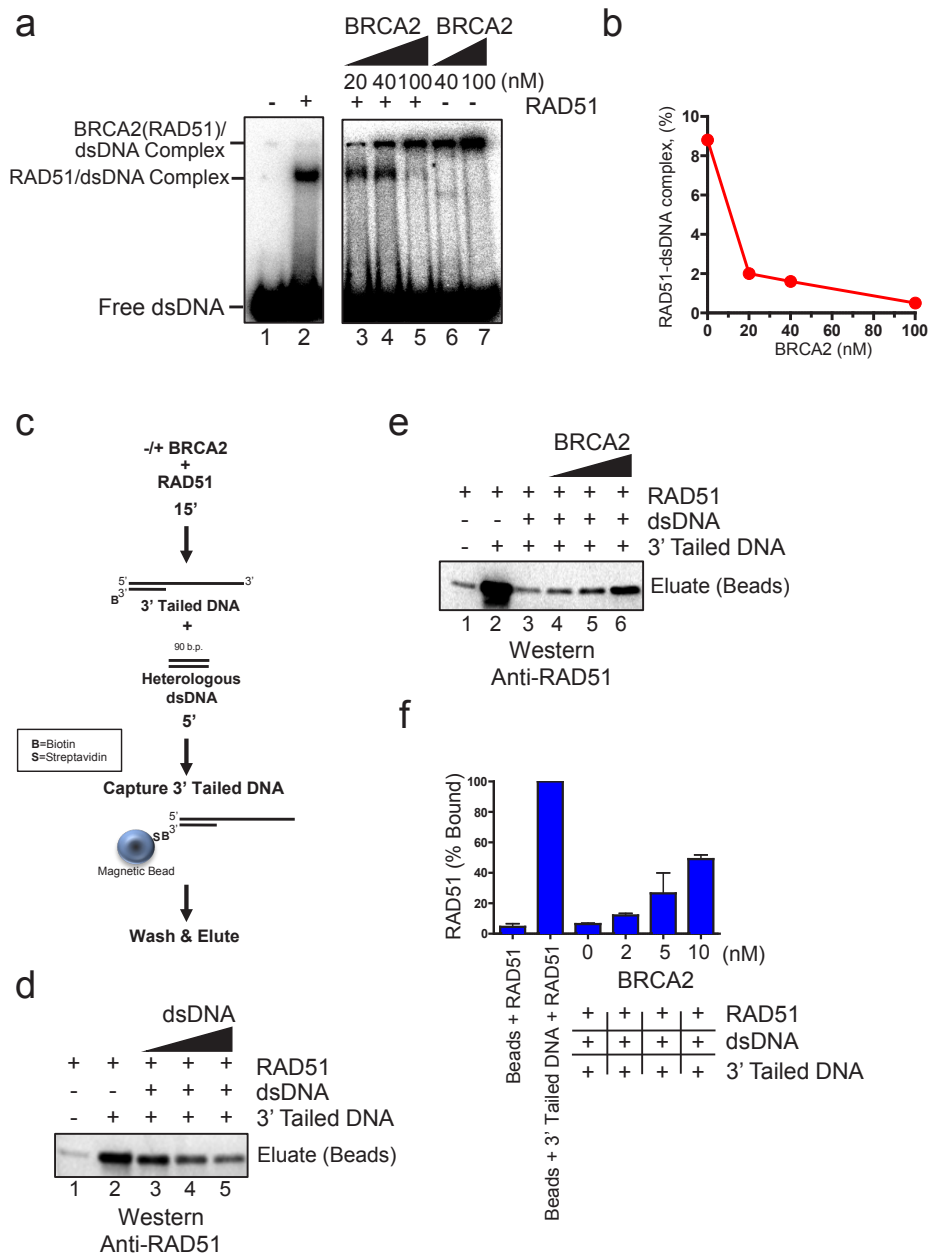
bars represent the S.D. **(d)** Quantification of the data in (b).



Supplementary Figure 7. DNA strand exchange controls. (a) In all DNA strand reactions shown: RPA is 0.1 μ M, RAD51 is 0.22 μ M, and BRCA2 is 40 nM. Lane 1: no protein control. Lane 2: RPA alone control. Lane 3: BRCA2 alone control. Lane 4: RAD51 alone. Lane 5: BRCA2 and RAD51. Lane 6: RPA and BRCA2. Lane 7: RPA first, RAD51 second. Lane 8: RPA first, BRCA2 and RAD51 second. Lane 9: RPA first, BRCA2 and RAD51 second, with 10-fold excess cold oligonucleotide complementary to the labeled pairing strand in the donor dsDNA present in the deproteinization step. Lane 10: RPA first, BRCA2 and RAD51 second using a heterologous labeled donor dsDNA. Lane 11: RPA first, BRCA2 and RAD51 second. Lane 12: Same reaction as in lane 11 with ATP omitted. **(b)** Quantification of the data in the autoradiogram in (a).

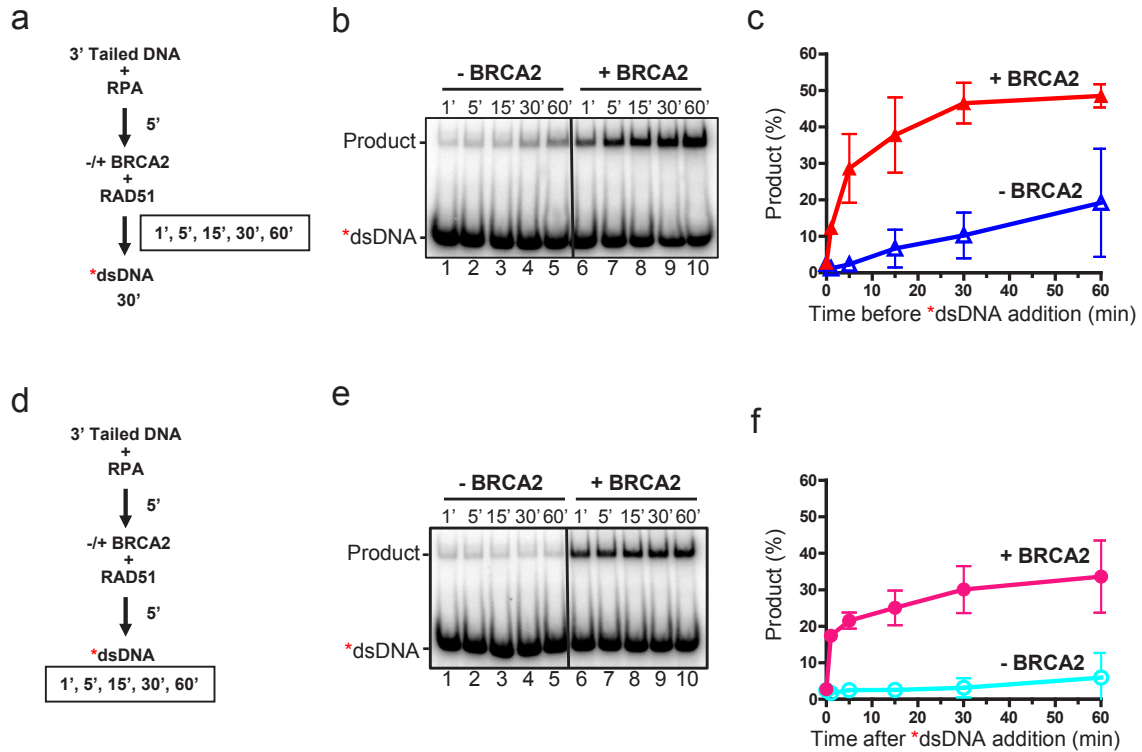


Supplementary Figure 8. BRCA2 stimulates DNA strand exchange in the presence of excess RAD51. (a) Scheme for DNA strand exchange reactions in the absence of RPA. The 3' tailed DNA substrate was incubated first with the indicated BRCA2 and RAD51 for 5 minutes at 37 °C, and then the radio-labeled dsDNA was added. (b) Autoradiogram of DNA strand exchange reactions, performed as described in (a), containing excess RAD51 (0.4 μM) in the presence of increasing concentrations of BRCA2.



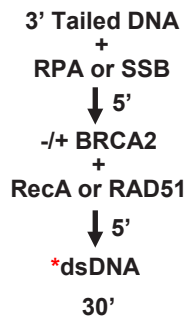
Supplementary Figure 9. BRCA2 prevents binding of RAD51 onto duplex DNA and targets RAD51 onto 3' Tailed DNA. (a) EMSA showing effect of BRCA2 on RAD51 binding to dsDNA. Increasing concentrations of BRCA2 were preincubated with 0.48 μ M RAD51 for 15 minutes at 37 $^{\circ}$ C prior to mixing with a 40 b.p. duplex DNA (4 nM molecules; the same dsDNA “RJ-Oligo1/RJ-Oligo2” used in the previous DNA strand exchange and EMSA analysis). The protein-DNA complexes were incubated for a further 30 minutes at 37 $^{\circ}$ C and resolved on a 6% TAE polyacrylamide gel. (b) Quantification of the band for the RAD51-dsDNA complex detected in (a). (c) Diagram of bead-capture experiment to measure binding of RAD51 to 3'

Tailed DNA in the presence competing heterologous dsDNA; proteins were mixed prior to their addition to the biotinylated 3' Tailed DNA and 90 b.p. dsDNA. **(d)** RAD51 (0.06 μ M) binding to biotinylated 3' Tailed DNA (0.2 nM molecules) either in the absence (lane 2) or presence (lanes 3-5) of excess dsDNA (1, 4, or 40 nM molecules respectively). **(e)** RAD51 (0.06 μ M) preincubated with or without increasing concentrations of BRCA2 for 15 minutes at 37 °C. The proteins were then incubated with the two DNA substrates for 5 minutes at 37 °C. **(f)** Quantification of the amount of RAD51 bound to the biotinylated 3' Tailed substrate. The amount of RAD51 bound to the 3' in the absence of dsDNA (panel e, lane 2) was set to a value of 100%.

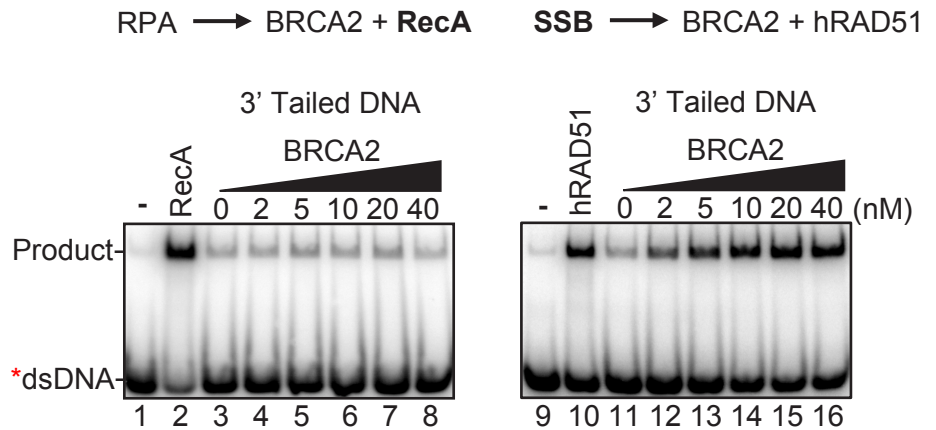


Supplementary Figure 10. Kinetic analyses. (a) Scheme for DNA strand exchange reactions indicating that assays were performed as in Figure 4 except that, after the addition of BRCA2 and RAD51, the proteins were incubated with the 3' tailed substrate from 1-60 minutes before addition of the labeled dsDNA to initiate the 30 minute reaction. (b) Autoradiogram of DNA strand exchange assays with 40 nM BRCA2 (+ BRCA2) or without (- BRCA2). (c) Quantification of (b). (d) In this reaction scheme, a time course from 1-60 minutes was performed after the addition of the labeled dsDNA. (e) Autoradiogram of the gel from reactions following the time course as described in (d) with 40 nM BRCA2 (+ BRCA2) or without BRCA2 (- BRCA2). (f) Quantification of the gel in (e). Error bars represent the S.D. from three independent experiments. A comparison of the linear regions of the time courses shows that presynaptic complex formation on RPA-ssDNA is increased ~20-fold by BRCA2. In contrast, when the time for presynaptic complex formation is held constant, but the time after addition of homologous dsDNA is varied, a steady differential throughout the time course of the reactions is seen. These kinetic analyses show that BRCA2 accelerates the rate of RAD51 nucleoprotein filament formation on ssDNA that is complexed with RPA, confirming the conclusions of the prior section.

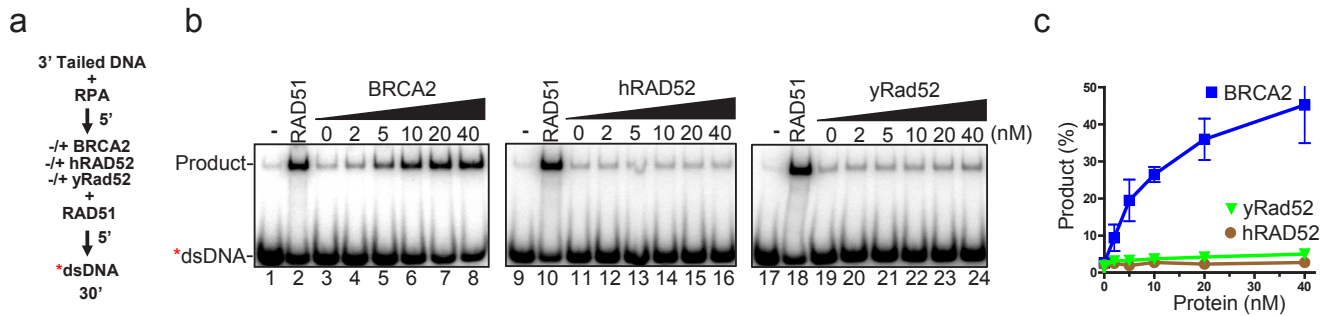
a



b



Supplementary Figure 11. Species specificity of DNA strand exchange. (a) Scheme for the DNA strand exchange reactions used in (b). (b) Left panel depicts an autoradiogram of assays performed as in (a) utilizing the 3' tailed substrate, except *E. coli* RecA (0.22 μ M) was substituted for RAD51. The right panel depicts an autoradiogram of reactions performed as in (a) except *E. coli* SSB (0.1 μ M) was substituted for RPA.



Supplementary Figure 12. Neither human RAD52 nor yeast Rad52 stimulates the DNA strand exchange activity of human RAD51 in the presence of RPA. (a) Scheme for the DNA strand exchange reactions used in (b) - (c). The 3' tailed DNA substrate was incubated first with RPA for 5 minutes, followed by BRCA2, human RAD52, or yeast Rad52. RAD51 was then added, followed by a 5 minute incubation, and finally the radio-labeled dsDNA was added to start the 30 minute reaction. (b) Autoradiograms of the assays comparing (left to right): BRCA2, human RAD52, or yeast Rad52. (c) Quantification of the gels shown in (b): BRCA2 (■), human RAD52 (●), or yeast Rad52 (▼). Error bars represent the S.D.